The impact of water vapor on CO_2 separation performance of mixed matrix membranes

Shinji Kanehashi,[1] George Chen,[1] Lachlan Ciddor,[2] Alan Chaffee[2] and Sandra E. Kentish*,[1]

[1] Peter Cook Centre for Carbon Capture and Storage, Department of Chemical and Biomolecular Engineering, The University of Melbourne, Victoria 3010, Australia

[2] School of Chemistry, Monash University, Victoria 3800, Australia

* Correspondence to Sandra E. Kentish

Tel : +61-3-8344-6682, Fax : +61-8344-4153

E-mail : sandraek@unimelb.edu.au

Abstract

A series of mixed matrix membranes (MMMs) using nanoparticles involving carbons, porous organic polymers and metal organic frameworks were prepared to investigate the impact of water vapor on CO_2 separation performance. The water uptake of MMMs using hydrophilic MOFs increased relative to more hydrophobic particles such as POP and carbons and this trend was reflected in the water vapor permeability, which varied by a factor of three between the hydrophobic and hydrophilic MMMs. These changes in water vapor permeability were strongly correlated with the water solubility, indicating that it is this solubility that is the controlling parameter. The calculated water diffusivity was consistent with previously published results. The gas permeability of MMMs in the presence of water vapor was also strongly affected by the nanoparticle hydrophobicity, with membranes composed of hydrophobic fillers out-performing hydrophilic fillers of comparable porosity. However in general, the differences in performance between MMMs and the pure polymer narrowed in the presence of water vapor.

Keywords: Water; Mixed matrix membrane; solubility; diffusivity; carbon capture

INTRODUCTION

Global warming has emerged as one of the serious environmental problems all over the world. This problem results from an increase in the emissions of greenhouse gases such as carbon dioxide (CO_2), methane, and perfluorocarbons to produce the requisite energy for our daily life. The separation of CO_2 from large emission sources such as power, iron and cement plants and its subsequent storage (*i.e.*, carbon capture and storage) would reduce the total CO_2 emissions [1, 2]. Applications for clean energy production involving hydrogen recovery[3, 4], natural gas sweetening [5, 6] and methane recovery from biogas [7] also require the separation of carbon dioxide and have received much attention in recent years. Polymeric membrane-based separation technology is an attractive approach to such gas/vapour separation due to its ease of operation, energy efficiency and cost-effectiveness, relative to absorption, adsorption, and cryogenic distillation, and has been applied in industrial applications [2, 8, 9]. However, minor components in the gas processing stream can have a large impact on the separation performance of these membranes [10]. In particular, water vapor is almost always present in industrial gas streams. This water vapor can cause a reduction in the CO_2 separation performance through competitive sorption and water clustering effects as the water molecules in the membrane occupy free volume that would otherwise be occupied by CO_2 [11, 12].

Generally, polymer membranes are easier to fabricate and more cost-effective than inorganic membranes. However, conventional polymeric membranes for gas separation have a typical tradeoff relationship between gas permeability and selectivity [13, 14]. An effective strategy to overcome this trade-off involves the use of polymer composites, so called mixed matrix membranes (MMMs), which combine the benefits of both polymer substrates and organic and/or inorganic fillers [15, 16]. MMMs have become attractive for gas separation applications in recent years not only because of their enhanced thermal, chemical,

and mechanical stability, but also their improved gas permeation/separation properties, when compared to homogeneous polymer membranes. To data, a large number of MMMs using carbon [17-21], zeolite [22-25], silica [26-30], metal organic frameworks (MOF) [31-33] and porous organic polymers (POP) [34] have been shown to be promising candidates for gas separation applications. Carbon materials are likely to be available at more moderate cost than other additives such as MOFs [35, 36]. MOFs and POPs have been widely investigated for gas storage and catalysis applications in recent years [37-41]. The stability of these materials is also of critical concern. For example, Zr (IV)-based MOFs such as UiO-66 [$Zr_6O_4(OH)_4(BDC)_6$] and its functionalized derivatives have been identified as more thermally and chemically stable than other MOFs [42]. In addition, UiO-66 has been shown to be very stable under 90RH% at 40°C, while surface degradation was observed in Cu-BTC under the same conditions [43]. These issues are further elaborated in a recent review paper [44]. Porous organic polymers (POPs) might be expected to be more hydrophobic and recently a triarylamine-based POP has indeed been shown to display a low water uptake [41]. In general, these MMMs are tested in isolation and are rarely compared to each other. Herein, a comparative study of the effect of water impact on the CO_2/CH_4 separation performance through various MMMs containing a variety of different nanoparticles involving, carbon, MOF, and POP has enabled important new insights into the factors that impact membrane performance. The use of processing conditions consistent with those that might be observed in natural gas or biogas processing provides an indication of membrane performance under such conditions [45].

EXPERIMENTAL

Materials

Aromatic polyimide, Matrimid®5218 (3,3,4,4-benzophenone tetracarboxylicdianhydride

diaminophenylidane) polyimide was purchased from Huntsman Advanced Materials Americas Inc, America for use as the host matrix. The Matrimid was purified by solution and re-precipitation using methanol (Analytical reagent, Chem-Supply, Australia) and dichloromethane (DCM, Analytical reagent, Chem-Supply, Australia). Graphitized mesoporous carbon (Carbon A), mesoporous carbon (Carbon B), and ZIF-8 (Basolite Z-1200) were purchased from Sigma-Aldrich Inc., America. Carbon C was produced from briquetted Victorian brown coal via mild steam activation at 800 °C for 90 min, in a fixed bed reactor under a flow of N_2/H_2O (3 L/min and 0.25 cm^3/min, respectively). POP-2 [46], Cu-BTC ($[Cu_3(BTC)_2]_3H_2O$, also known as HKUST-1 where BTC = benzene-1,3,5-tricarboxylate) [47], and UiO-66 [48] were synthesized in house according to the previous literature. All polyimide and commercial nanoparticles were dried at 100°C overnight under vacuum to remove moisture before use.

Membrane Preparation

Pure Matrimid and MMMs were prepared by a solvent casting method. The loading of nanoparticle was calculated based on the following equation;

$$\text{Filler loading (wt\%)} = \frac{w_{filler}}{w_{polymer} + w_{filler}} \times 100 \quad (1)$$

where $w_{polymer}$ and w_{filler} are weight of polymer and filler, respectively. DCM solutions of 3-4 wt% filler and polymer were separately prepared. These separate solutions were stirred overnight at room temperature and then sonicated (Unisonics, Australia) for 30 minutes within an ice bath. The well dispersed solutions were mixed together and then again treated by physical stirring overnight and ultrasonication for 30 minutes. Base Matrimid membranes and mixed matrix membranes of different filler loadings (*e.g.* 10, 20, and 30 wt%) were prepared from such solutions by a standard casting method [49]. A homogeneous polymer/filler solution was cast onto a glass petri dish which was covered to prevent

contamination and left at room temperature for 24-48 hours. The homogeneous membranes were then removed from the petri dish using a small amount of distilled water. The membrane was placed in a vacuum oven at 35°C for 24 hours and further dried at 100°C for 24 hours. The thickness of the well-dried membrane was on average 80 μm, as measured by a micrometer (IP65, Mitsutoyo, Japan), giving an accuracy of ± 1 μm.

Characterization

Nitrogen adsorption–desorption measurements of the nanoparticles was conducted on a ASAP2010 (Micromeritics, USA) apparatus at 77 K. The internal surface area was then calculated by the BET method [50]. The particle size distribution of the nanoparticles was measured by dynamic light scattering (DLS) using a Zetasizer 2000 (Malvern, UK) instrument. The membrane density (ρ) was determined based on the Archimedean principle using an analytical balance (Mettler Toledo AB204-5) at room temperature (23 ± 1°C) [51], The water uptake of the membrane was determined by immersion in purified water at 35 ± 1°C until equiribrium water sorption was attained. The water uptake was calculated based on the following equation;

$$\text{Water uptake (wt\%)} = \frac{w_{wet} - w_{dry}}{w_{dry}} \times 100 \quad (2)$$

where w_{wet} and w_{dry} are the weight of a water-swollen membrane at equilibrium state and a well-dried membrane respectively.

Dry and humidified gas permeability in mixtures of 10% CO_2 in CH_4 were determined at 35 °C and 7.5 bar by a constant pressure variable volume apparatus designed and built in-house [12]. For all gas permeability measurements helium was used as a sweep gas on the permeate side. CO_2 and CH_4 permeabilities were determined through a mass flowmeter (GFC mass flowmeter, Aalborg, USA), and gas chromatography (CP-3800, Varian, Inc., Australia). Water permeability was also measured through humidity probes (HMT, Probe

type 334 Vaisala Oyj, Finland) on the feed and permeate side. Concentration polarization can readily occur under humidified conditions due to the formation of a concentration gradient at either surface of the membrane, as water permeates much faster than other gases [12, 45, 52, 53]. To eliminate these effects in the present work, stainless steel wool was placed on both sides of the membrane to increase turbulence within the boundary layer. Further, the feed and sweep permeate flowrates were increased to a point where the measurement was independent of this parameter. Under these conditions, the water vapor concentration on the membrane surface approaches the bulk concentration. In the present case, a feed flowrate of 1.6 L/min and a helium sweep gas flowrate of 50 ml/min was used to eliminate such concentration polarization. The water activity, α or relative humidity was determined by

$$\alpha = \frac{p_{H_2O}}{p_{sat}} \tag{3}$$

where p_{H2O} is the water vapor partial pressure and p_{sat} the saturation water vapor pressure at 35^{o}C (5.64 kPa).

RESULTS AND DISCUSSION

Characterization

The nanoparticle properties are summarized in Table 1. The crystal density of the nanoparticles is cited from manufacturer information and the literature [33, 54-56]. The surface area increases with increasing pore volume, consistent with data reported for MOFs and carbon aerogels [57, 58]. The membrane density of pure Matrimid and 20 wt% MMMs are summarized in Table 2. The density of pure Matrimid was 1.223 g/cm^3, which is in good agreement with the literature value [59]. The fractional free volume (*FFV*) in each membrane can be determined from the density of the membrane, the base polymer and the nanoparticles using a previously established method [60] and this data is also presented in

Table 2. We have previously shown that the permeability of pure single gases through these membranes can be correlated directly to this *FFV* value, suggesting that the gas transport mechanism of these MMMs at low feed pressure is controlled by the gas diffusivity [60].

Figure 1 presents the water uptake values of MMMs as a function of filler loading, while Figure 2 shows how this uptake varies with pore volume. The water uptake value of pure Matrimid is 2.8 wt% at 35°C which is in good agreement with the reported value [61]. The water uptake of the MMMs reflects the nature of the fillers with the water uptake values for Carbon A and for POP-2 membranes below that of the host matrix. On the other hand, the water uptake of other membranes increased with increasing filler loading. The highest water uptake was observed in Cu-BTC and in UiO-66, related to the high porosity of these materials (Table 1 and Figure 2) and the presence of hydroxyl groups coordinated into each structure [43, 44]. The pore volume for the hydrophobic ZIF-8 and POP-2 materials is less important, with little correlation with this parameter seen in Figure 2. Changes in pore volume probably contribute to the differences in water uptake for the three carbon materials. Water uptake in activated carbon materials is usually related to a combination of both pore volume and the extent of surface oxide functionalization [62, 63].

Water vapor permeation and its impact

Figure 3 presents the water vapor permeability through the MMMs compared to the base polymer, Matrimid. As has been observed previously, the water vapor permeability of Matrimid increases as water activity increases, ranging from 3200 to 3750 in CH_4 and from 3650 to 3900 in 10% CO_2 in CH_4. This increase is generally related to the increase in the water vapor solubility at higher humidities [12, 64, 65]. In addition, the water vapor permeability of all membranes in a stream of 10% CO_2 in CH_4 at a water activity of 0.8 is about 10% higher than that in a pure CH_4 gas. This is because the CO_2 induces some

membrane plasticization. The water permeability of the MMMs at these humidities varied from 2800 to 9400 barrer in humidified CH_4, and from 2900 to 10000 barrer in 10% CO_2 in CH_4; giving an over threefold difference in permeability between the hydrophobic and hydrophilic MMMs. This data is plotted on a Robeson's plot for H_2O/CO_2 in Figure 4. The slope of the theoretical upper bound of H_2O/CO_2 is calculated using the approach from Freeman (1999) [14]. The Matrimid-based MMMs exist below the upper bound for these gas pairs, which is similar to the performance of other aromatic polyimides.

It should be noted that this data is collected with a dry sweep gas, so that the water concentration within the membrane varies significantly across the cross-section. In turn, this means that the degree of plasticization of the Matrimid matrix and the extent of water clustering also varies. As noted by Koester *et al*., increases in the permeate humidity will change the nature of both plasticization and clustering and will likely lead to changes in the data [52]. Similarly, changes to the thickness of the membrane could also change the recorded permeability [66]. However, the influence of the nanoparticle within the mixed matrix structure should remain unaffected.

It should also be noted that these results are recorded in a gas stream that contains relatively low partial pressures of carbon dioxide. At higher partial pressures, the water permeability through the Matrimid matrix is likely to increase, particularly at lower water humidities, reflecting additional plasticization or swelling from this gas [12]. In turn, this is likely to lead to an overall increase in the MMM permeability.

The water vapor permeability of the 20 wt% MMMs at $\alpha = 0.8$ is strongly correlated with the water uptake (water vapor solubility at $\alpha = 1.0$) as presented in Figure 5. This graph shows that there is a linear relationship between the water permeability (P) and the water solubility (S). If the permeability can be described by the simple relationship $P = D \times S$, then the gradient of this line can be considered as an estimate of the water diffusivity in these

systems. Indeed, the calculated values of this gradient ($3.41 \pm 0.15 \times 10^{-8}$ cm^2/s in pure CH_4 and $3.63 \pm 0.16 \times 10^{-8}$ cm^2/s in 10% CO_2 in CH_4) are highly consistent with previously published values of the water permeability through pure Matrimid at $\alpha = 0.8$ (3.05×10^{-8} cm^2/s) [11]. This result suggests that the water vapor permeability through Matrimid-based MMMs is determined by the water vapor solubility rather than the diffusivity. This result is in contrast to our previous work which showed that the permeability of light gases such as CH_4 and CO_2 was dominated by the diffusivity, with increases in permeability directly correlated with increases in free volume [60]. The slight increase in diffusivity for 10% CO_2 in CH_4 relative to pure CH_4 may result from CO_2 induced plasticization, although the difference is within the experimental error margin.

Figure 6 presents the CO_2 and CH_4 permeability, and CO_2/CH_4 selectivity under humidified conditions at 35°C for each MMM. As has been previously described, the water vapor causes a loss of both permeability and selectivity for these light gases in pure Matrimid, due to a combination of competitive sorption and water clustering (antiplasticisation), which reduces the diffusivity of the gases [11]. In the present case, the loss of permeability is greater for the more hydrophilic MMMs such as Cu-BTC, UiO-66, and ZIF-8, while that for the hydrophobic POP-2 and carbon nanoparticles is less. These changes in the gas permeability again reflect changes in the water solubility, which affect the extent of both competitive sorption and water clustering. The changes in CO_2/CH_4 selectivity for all membranes is of the order of 10% of the base value and within experimental error, no clear trend can be established.

The net impact of water on the Robeson's plot for CO_2/CH_4 is provided in Figure 7. While MMMs with the highly porous Cu-BTC provide the best performance in a dry system, this behaviour is reversed once water is added. Under these circumstances, the more hydrophobic, but still porous filler materials, such as POP-2, Carbon C and ZIF-8 provide

better results. The poorest performance is provided by materials that are either hydrophilic or lacking in free volume. In general, the performance of all MMMs is closer to that of pure Matrimid and hence it may be difficult to justify the added expense of manufacturing these materials relative to a simple polymer.

CONCLUSIONS

Matrimid-based MMMs using a range of nanoparticles were prepared and tested in the presence of water vapor. Incorporation of hydrophobic nanoparticles such as Carbon A and POP-2 into the polyimide matrix decreased the water uptake values, suggesting that the membranes were becoming more hydrophobic. A linear correlation was observed between the water vapor permeability of MMMs and the water vapor solubility and the gradient of this line indicated a water diffusivity consistent with published results. The presence of water vapor in the feed gas leads to a drop of gas permeability of all MMMs, however, the impact is less for the more hydrophobic materials. These results suggest that MMMs prepared using highly porous, hydrophobic nanoparticles can be effective in gas separation applications such as natural gas sweetening, biogas purification and post-combustion carbon capture, when water vapor is present as an impurity. However, the advantages of a MMM reduce in these circumstances and a case to prepare these more complicated structures would need to be carefully assessed.

ACKNOWLEDGEMENT

This research was supported by the Scientific and Industry Endowment Fund in Australia (SIEF Grant ID RP02-035) and a Grant-in-Aid for the Japan Society for the Promotion of Science Fellows (JSPS Grant ID 2410856).

REFERENCES

[1] M. Mikkelsen, M. Jorgensen, F.C. Krebs, The teraton challenge. A review of fixation and transformation of carbon dioxide, Energy Environ. Sci., 3 (2010) 43-81.

[2] T.C. Merkel, H. Lin, X. Wei, R. Baker, Power plant post-combustion carbon dioxide capture: An opportunity for membranes, J. Membr. Sci., 359 (2010) 126-139.

[3] T. Yang, T.-S. Chung, High performance ZIF-8/PBI nano-composite membranes for high temperature hydrogen separation consisting of carbon monoxide and water vapor, Int. J. Hydrogen Energy, 38 (2013) 229-239.

[4] T. Yang, Y. Xiao, T.-S. Chung, Poly-/metal-benzimidazole nano-composite membranes for hydrogen purification, Energy Environ. Sci., 4 (2011) 4171-4180.

[5] R.W. Baker, K. Lokhandwala, Natural gas processing with membranes: an overview, Ind. Eng. Chem. Res., 47 (2008) 2109-2121.

[6] C.A. Scholes, G.W. Stevens, S.E. Kentish, Membrane gas separation applications in natural gas processing, Fuel, 96 (2012) 15-28.

[7] S. Basu, A.L. Khan, A. Cano-Odena, C. Liu, I.F.J. Vankelecom, Membrane-based technologies for biogas separations, Chem. Soc. Rev., 39 (2010) 750-768.

[8] R.W. Baker, Membrane Technology and Applications, McGraw-Hill, New York, 2000.

[9] B.D. Freeman, Y. Yampolskii, Membrane Gas Separation, John Wiley & Sons, West Sussex, 2010.

[10] C.A. Scholes, S.E. Kentish, G.W. Stevens, Effects of minor components in carbon dioxide capture using polymeric gas separation membranes, Sep. Purif. Rev., 38 (2009) 1-44.

[11] G.Q. Chen, C.A. Scholes, C.M. Doherty, A.J. Hill, G.G. Qiao, S.E. Kentish, Modeling of the sorption and transport properties of water vapor in polyimide membranes, J. Membr. Sci., 409–410 (2012) 96-104.

[12] G.Q. Chen, C.A. Scholes, G.G. Qiao, S.E. Kentish, Water vapor permeation in polyimide membranes, J. Membr. Sci., 379 (2011) 479-487.

[13] L.M. Robeson, The upper bound revisited, J. Membr. Sci., 320 (2008) 390-400.

[14] B.D. Freeman, Basis of Permeability/Selectivity Tradeoff Relations in Polymeric Gas Separation Membranes, Macromolecules, 32 (1999) 375-380.

[15] G. Dong, H. Li, V. Chen, Challenges and opportunities for mixed-matrix membranes for gas separation, J. Mat. Chem. A, 1 (2013) 4610-4630.

[16] M. Rezakazemi, A. Ebadi Amooghin, M.M. Montazer-Rahmati, A.F. Ismail, T. Matsuura, State-of-the-art membrane based CO2 separation using mixed matrix membranes (MMMs): An overview on current status and future directions, Prog. Polym. Sci., 39 (2014) 817-861.

[17] D.Q. Vu, W.J. Koros, S.J. Miller, Mixed matrix membranes using carbon molecular sieves: I. Preparation and experimental results, J. Membr. Sci., 211 (2003) 311-334.

[18] M. Anson, J. Marchese, E. Garis, N. Ochoa, C. Pagliero, ABS copolymer-activated carbon mixed matrix membranes for CO2/CH4 separation, J. Membr. Sci., 243 (2004) 19-28.

[19] A. Singh, W.J. Koros, Significance of entropic selectivity for advanced gas separation membranes, Ind. Eng. Chem. Res., 35 (1996) 1231-1234.
[20] J. Marchese, M. Anson, N.A. Ochoa, P. Prádanos, L. Palacio, A. Hernández, Morphology and structure of ABS membranes filled with two different activated carbons, Chem. Eng. Sci., 61 (2006) 5448-5454.
[21] M.G. García, J. Marchese, N.A. Ochoa, High activated carbon loading mixed matrix membranes for gas separations, J Mater Sci, 47 (2012) 3064-3075.
[22] M. Rostamizadeh, M. Rezakazemi, K. Shahidi, T. Mohammadi, Gas permeation through H2-selective mixed matrix membranes: Experimental and neural network modeling, Int. J. Hydrogen Energy, 38 (2013) 1128-1135.
[23] R. Mahajan, W.J. Koros, Mixed matrix membrane materials with glassy polymers. Part 1, Polym. Eng. Sci., 42 (2002) 1420-1431.
[24] S. Kanehashi, H. Gu, R. Shindo, S. Sato, T. Miyakoshi, K. Nagai, Gas permeation and separation properties of polyimide/ZSM-5 zeolite composite membranes containing liquid sulfolane, J. Appl. Polym. Sci., Accepted (2012).
[25] Y. Zhang, K.J. Balkus Jr., I.H. Musselman, J.P. Ferraris, Mixed-matrix membranes composed of Matrimid® and mesoporous ZSM-5 nanoparticles, J. Membr. Sci., 325 (2008) 28-39.
[26] T.C. Merkel, B.D. Freeman, R.J. Spontak, Z. He, I. Pinnau, P. Meakin, A.J. Hill, Ultrapermeable, reverse-selective nanocomposite membranes, Science, 296 (2002) 519-522.
[27] Z. He, I. Pinnau, A. Morisato, Nanostructured poly(4-methyl-2-pentyne)/silica hybrid membranes for gas separation, Desalination, 146 (2002) 11-15.
[28] T.C. Merkel, B.D. Freeman, R.J. Spontak, Z. He, I. Pinnau, P. Meakin, A.J. Hill, Sorption, transport, and structural evidence for enhanced free volume in poly(4-methyl-2-pentyne)/fumed silica nanocomposite membranes, Chem. Mat., 15 (2002) 109-123.
[29] B.D. Reid, F.A. Ruiz-Trevino, I.H. Musselman, K.J. Balkus, J.P. Ferraris, Gas permeability properties of polysulfone membranes containing the mesoporous molecular sieve MCM-41, Chem. Mat., 13 (2001) 2366-2373.
[30] S. Kim, E. Marand, J. Ida, V.V. Guliants, Polysulfone and mesoporous molecular sieve MCM-48 mixed matrix membranes for gas separation, Chem. Mat., 18 (2006) 1149-1155.
[31] S. Japip, H. Wang, Y. Xiao, T. Shung Chung, Highly permeable zeolitic imidazolate framework (ZIF)-71 nano-particles enhanced polyimide membranes for gas separation, J. Membr. Sci., 467 (2014) 162-174.
[32] L. Ge, W. Zhou, V. Rudolph, Z. Zhu, Mixed matrix membranes incorporated with size-reduced Cu-BTC for improved gas separation, J. Mat. Chem. A, 1 (2013) 6350-6358.
[33] Q. Song, S.K. Nataraj, M.V. Roussenova, J.C. Tan, D.J. Hughes, W. Li, P. Bourgoin, M.A. Alam, A.K. Cheetham, S.A. Al-Muhtaseb, E. Sivaniah, Zeolitic imidazolate framework (ZIF-8) based polymer nanocomposite membranes for gas separation, Energy Environ. Sci., 5

(2012) 8359-8369.
[34] H. Zhao, Z. Jin, H. Su, J. Zhang, X. Yao, H. Zhao, G. Zhu, Target synthesis of a novel porous aromatic framework and its highly selective separation of CO2/CH4, Chem. Comm., 49 (2013) 2780-2782.
[35] J. Wang, L. Huang, R. Yang, Z. Zhang, J. Wu, Y. Gao, Q. Wang, D. O'Hare, Z. Zhong, Recent advances in solid sorbents for CO2 capture and new development trends, Energy Environ. Sci., (2014).
[36] M. Sevilla, R. Mokaya, Energy storage applications of activated carbons: supercapacitors and hydrogen storage, Energy Environ. Sci., 7 (2014) 1250-1280.
[37] J.-R. Li, J. Sculley, H.-C. Zhou, Metal–Organic Frameworks for Separations, Chem. Rev., 112 (2011) 869-932.
[38] K. Sumida, D.L. Rogow, J.A. Mason, T.M. McDonald, E.D. Bloch, Z.R. Herm, T.-H. Bae, J.R. Long, Carbon dioxide capture in metal–organic frameworks, Chem. Rev., 112 (2011) 724-781.
[39] Z. Zhang, Z.-Z. Yao, S. Xiang, B. Chen, Perspective of microporous metal-organic frameworks for CO2 capture and separation, Energy Environ. Sci., 7 (2014) 2868-2899.
[40] J. Liu, P.K. Thallapally, B.P. McGrail, D.R. Brown, J. Liu, Progress in adsorption-based CO2 capture by metal-organic frameworks, Chem. Soc. Rev., 41 (2012) 2308-2322.
[41] C. Hua, A. Rawal, T.B. Faust, P.D. Southon, R. Babarao, J.M. Hook, D.M. D'Alessandro, Exploiting stable radical states for multifunctional properties in triarylamine-based porous organic polymers, J. Mat. Chem. A, 2 (2014) 12466-12474.
[42] J.H. Cavka, S. Jakobsen, U. Olsbye, N. Guillou, C. Lamberti, S. Bordiga, K.P. Lillerud, A new zirconium inorganic building brick forming metal organic frameworks with exceptional stability, J. Am. Chem. Soc., 130 (2008) 13850-13851.
[43] J.B. DeCoste, G.W. Peterson, B.J. Schindler, K.L. Killops, M.A. Browe, J.J. Mahle, The effect of water adsorption on the structure of the carboxylate containing metal-organic frameworks Cu-BTC, Mg-MOF-74, and UiO-66, J. Mat. Chem. A, 1 (2013) 11922-11932.
[44] N.C. Burtch, H. Jasuja, K.S. Walton, Water stability and adsorption in metal–organic frameworks, Chem. Rev., 114 (2014) 10575-10612.
[45] G.Q. Chen, S. Kanehashi, C.M. Doherty, A.J. Hill, S.E. Kentish, Water vapor permeation through cellulose acetate membranes and its impact upon membrane separation performance for natural gas purification, J. Membr. Sci., 487 (2015) 249-255.
[46] D. Hua, Y.K. Ong, Y. Wang, T. Yang, T.-S. Chung, ZIF-90/P84 mixed matrix membranes for pervaporation dehydration of isopropanol, J. Membr. Sci., 453 (2014) 155-167.
[47] B. Xiao, Q. Yuan, R.A. Williams, Exceptional function of nanoporous metal organic framework particles in emulsion stabilisation, Chem. Comm., 49 (2013) 8208-8210.
[48] K. Tulig, K.S. Walton, An alternative UiO-66 synthesis for HCl-sensitive nanoparticle encapsulation, RSC Adv., 4 (2014) 51080-51083.
[49] M. Valero, B. Zornoza, C. Téllez, J. Coronas, Mixed matrix membranes for gas

separation by combination of silica MCM-41 and MOF NH2-MIL-53(Al) in glassy polymers, Microporous Mesoporous Mater., 192 (2014) 23-28.
[50] S. Brunauer, P.H. Emmett, E. Teller, Adsorption of gases in multimolecular layers, J. Am. Chem. Soc., 60 (1938) 309-319.
[51] G.Q. Chen, C.A. Scholes, C.M. Doherty, A.J. Hill, G.G. Qiao, S.E. Kentish, The thickness dependence of Matrimid films in water vapor permeation, Chem. Eng. J., 209 (2012) 301-312.
[52] S. Koester, F. Roghmans, M. Wessling, Water vapor permeance: The interplay of feed and permeate activity, J. Membr. Sci., 485 (2015) 69-78.
[53] S.J. Metz, W.J.C. van de Ven, J. Potreck, M.H.V. Mulder, M. Wessling, Transport of water vapor and inert gas mixtures through highly selective and highly permeable polymer membranes, J. Membr. Sci., 251 (2005) 29-41.
[54] S.S.-Y. Chui, S.M.-F. Lo, J.P.H. Charmant, A.G. Orpen, I.D. Williams, A chemically functionalizable nanoporous material [Cu3(TMA)2(H2O)3]n, Science, 283 (1999) 1148-1150.
[55] S. Basu, A. Cano-Odena, I.F.J. Vankelecom, Asymmetric Matrimid®/[Cu3(BTC)2] mixed-matrix membranes for gas separations, J. Membr. Sci., 362 (2010) 478-487.
[56] I. Senkovska, S. Kaskel, High pressure methane adsorption in the metal-organic frameworks Cu3(btc)2, Zn2(bdc)2dabco, and Cr3F(H2O)2O(bdc)3, Microporous Mesoporous Mater., 112 (2008) 108-115.
[57] Y. Ming, J. Purewal, D.a. Liu, A. Sudik, C. Xu, J. Yang, M. Veenstra, K. Rhodes, R. Soltis, J. Warner, M. Gaab, U. Müller, D.J. Siegel, Thermophysical properties of MOF-5 powders, Microporous Mesoporous Mater., 185 (2014) 235-244.
[58] C. Scherdel, G. Reichenauer, M. Wiener, Relationship between pore volumes and surface areas derived from the evaluation of N2-sorption data by DR-, BET- and t-plot, Microporous Mesoporous Mater., 132 (2010) 572-575.
[59] T.-S. Chung, S.S. Chan, R. Wang, Z. Lu, C. He, Characterization of permeability and sorption in Matrimid/C60 mixed matrix membranes, J. Membr. Sci., 211 (2003) 91-99.
[60] S. Kanehashi, G.Q. Chen, C.A. Scholes, B. Ozcelik, C. Hua, L. Ciddor, P.D. Southon, D.M. D'Alessandro, S.E. Kentish, Enhancing gas permeability in mixed matrix membranes through tuning the nanoparticle properties, J. Membr. Sci., 482 (2015) 49-55.
[61] B.W. Rowe, B.D. Freeman, D.R. Paul, Effect of sorbed water and temperature on the optical properties and density of thin glassy polymer films on a silicon substrate, Macromolecules, 40 (2007) 2806-2813.
[62] E. Dimotakis, M. Cal, J. Economy, M. Rood, S. Larson, Water Vapor Adsorption on Chemically Treated Activated Carbon Cloths, Chemistry of Materials, 7 (1995) 2269-2272.
[63] S.S. Barton, J.E. Koresh, Adsorption interaction of water with microporous adsorbents. Part 1.-Water-vapour adsorption on activated carbon cloth, Journal of the Chemical Society, Faraday Transactions 1: Physical Chemistry in Condensed Phases, 79 (1983) 1147-1155.
[64] J. Potreck, K. Nijmeijer, T. Kosinski, M. Wessling, Mixed water vapor/gas transport

through the rubbery polymer PEBAX® 1074, J. Membr. Sci., 338 (2009) 11-16.
[65] H. Sijbesma, K. Nymeijer, R. van Marwijk, R. Heijboer, J. Potreck, M. Wessling, Flue gas dehydration using polymer membranes, J. Membr. Sci., 313 (2008) 263-276.
[66] H. Azher, C.A. Scholes, G.W. Stevens, S.E. Kentish, Water permeation and sorption properties of Nafion 115 at elevated temperatures, J. Membr. Sci., 459 (2014) 104-113.

Figure Captions

Fig. 1. Liquid water uptake of MMMs at 35°C, as a function of filler loading.

Fig. 2. Liquid water uptake of MMMs at 35°C, as a function of pore volume of the nanoparticles.

Fig. 3. Water vapor permeability of Matrimid and 20wt% MMMs at water activity of 0.8, at 35°C. The balance gas is (a) CH_4 and (b) mixed 10% CO_2 in CH_4.

Fig. 4. Robeson′s plot of water vapor (H_2O) against CO_2 in polymeric membranes, highlighting the position of pure Matimid (PI) and 20wt% MMMs relative to the upper bound.

Fig. 5. Water vapor permeability of 20 wt% MMMs at water activity of 0.8 as a function of water vapor solubility (at a water activity of 1.0).

Fig. 6. (a) CO_2 and (b) CH_4 permeability, and (c) CO_2/CH_4 selectivity of 20 wt% MMMs at water activity of 0.8 at 35°C, relative to that of the same membrane in a dry gas. The balance gas is mixed 10% CO_2 in CH_4.

Fig. 7. CO_2/CH_4 separation performance of 20 wt% MMMs at (a) dry pure gas (b) dry mixed 10% CO_2 in CH_4, and (c) humidified mixed 10% CO_2 in CH_4 at 35°C.

Table Captions

Table 1 Physical properties of the nanoparticles

Table 2 Physical properties of pure Matrimid and 20 wt% Mixed Matrix Membranes

Figure 1

Click here to download high resolution image

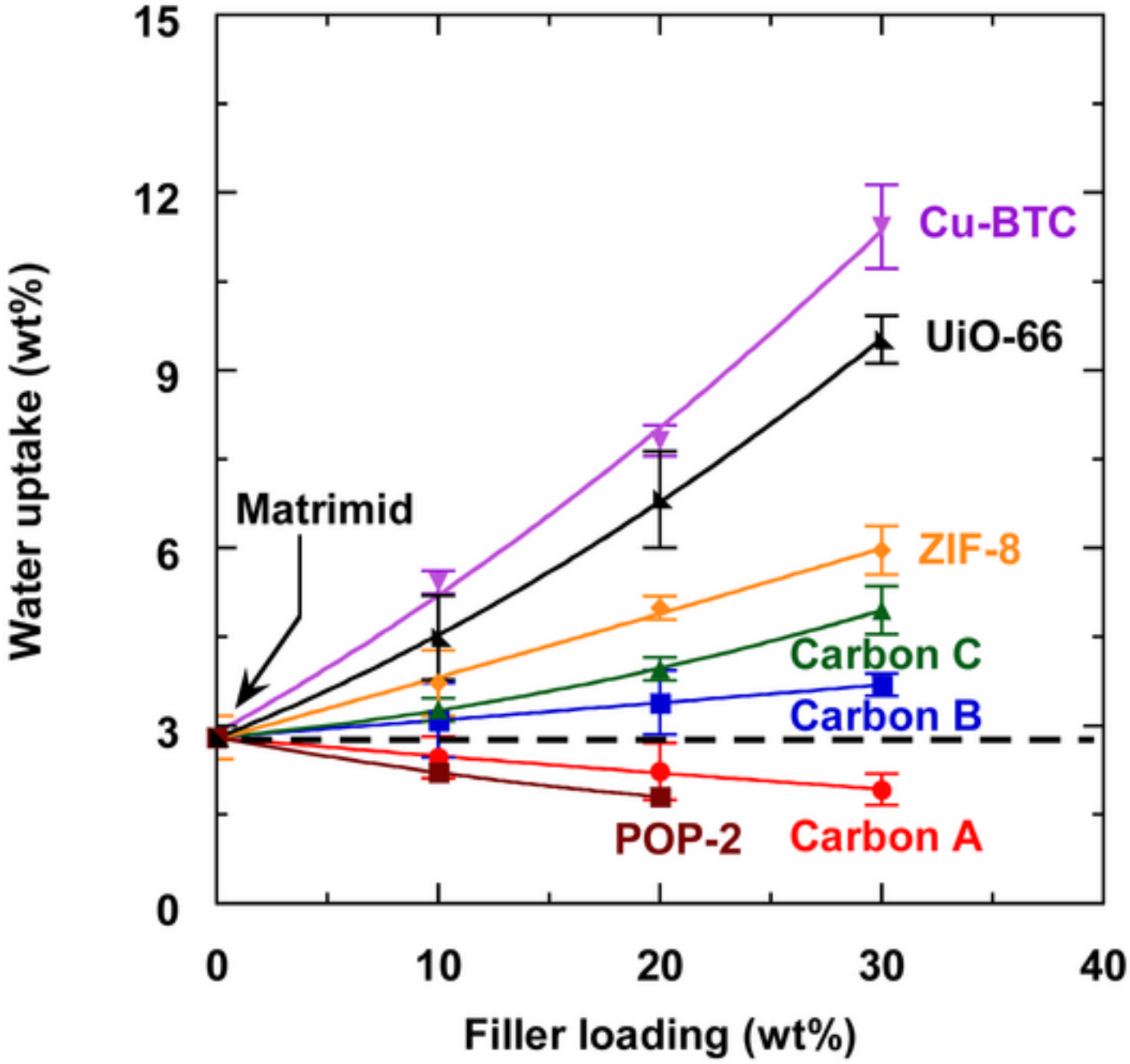

Figure 2

Click here to download high resolution image

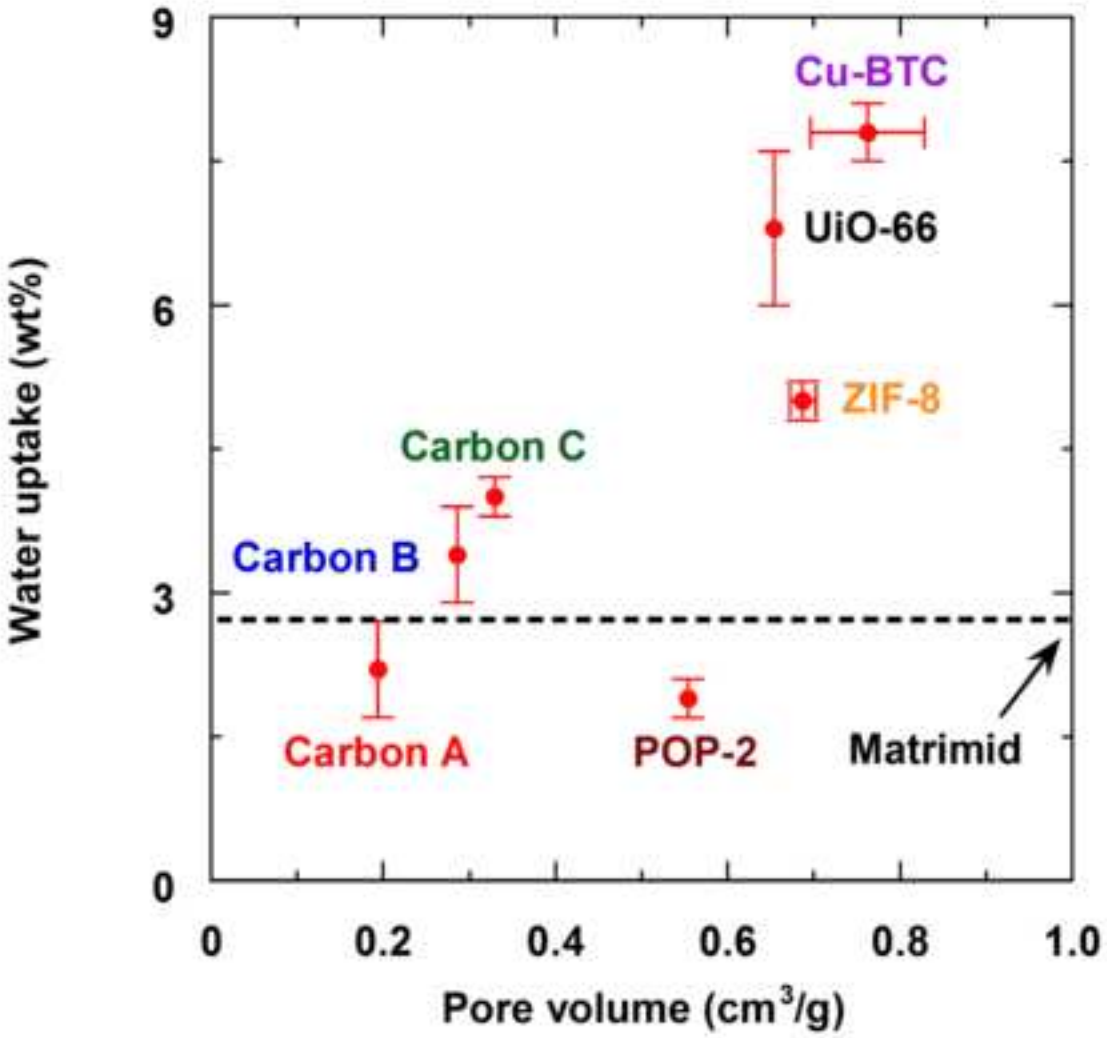

Figure 3

Click here to download high resolution image

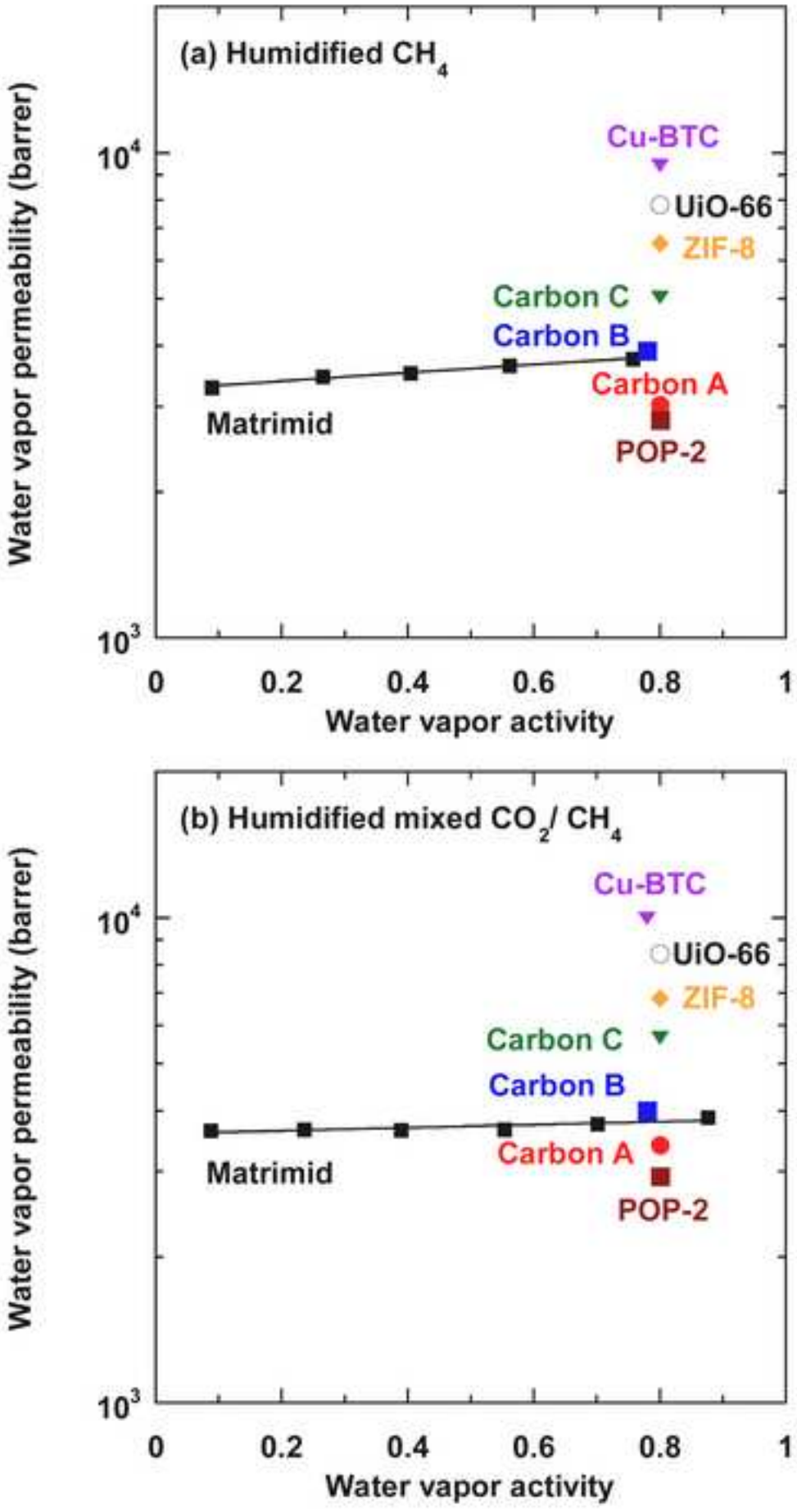

Figure 4

Click here to download high resolution image

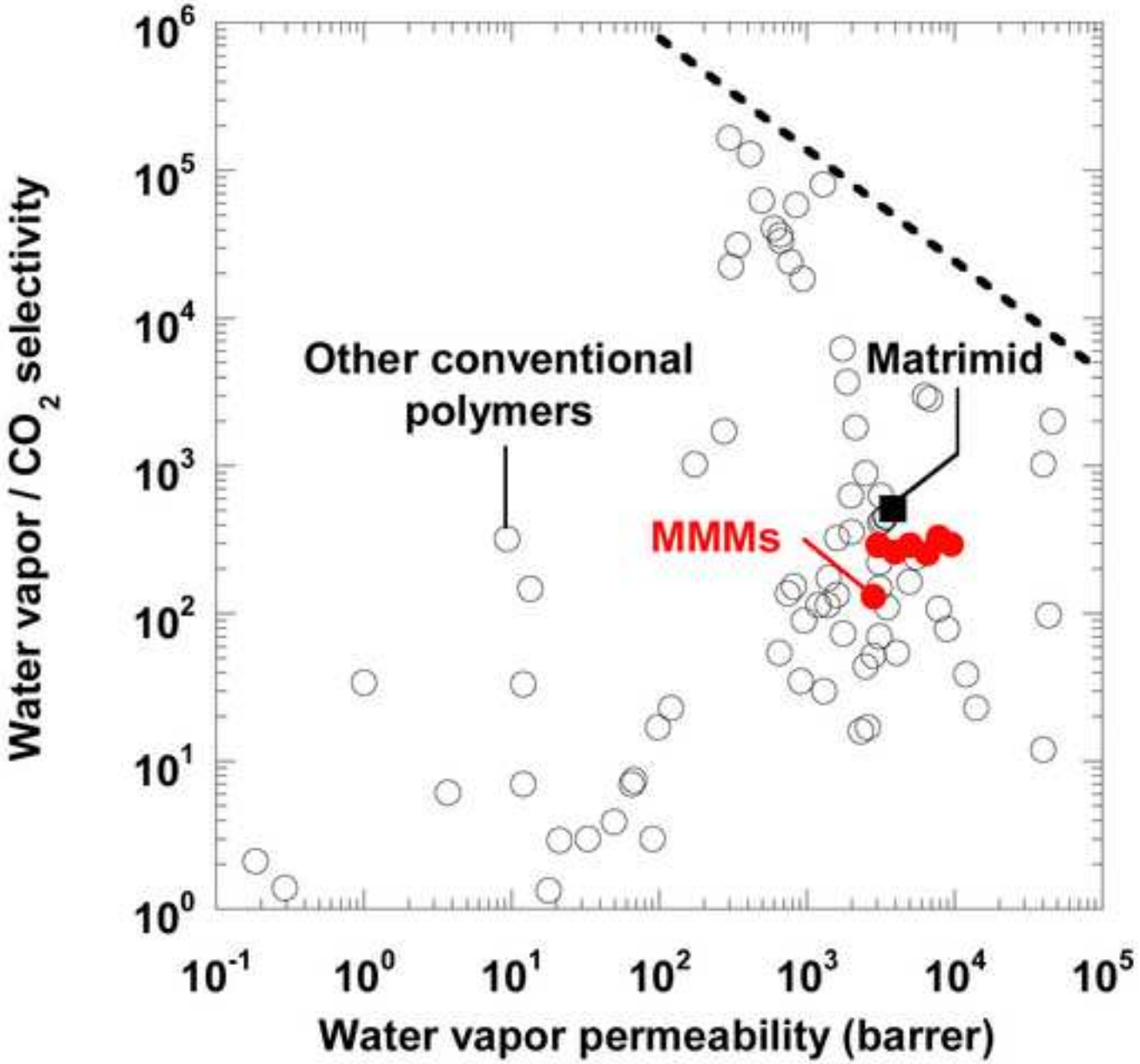

Figure 5

Click here to download high resolution image

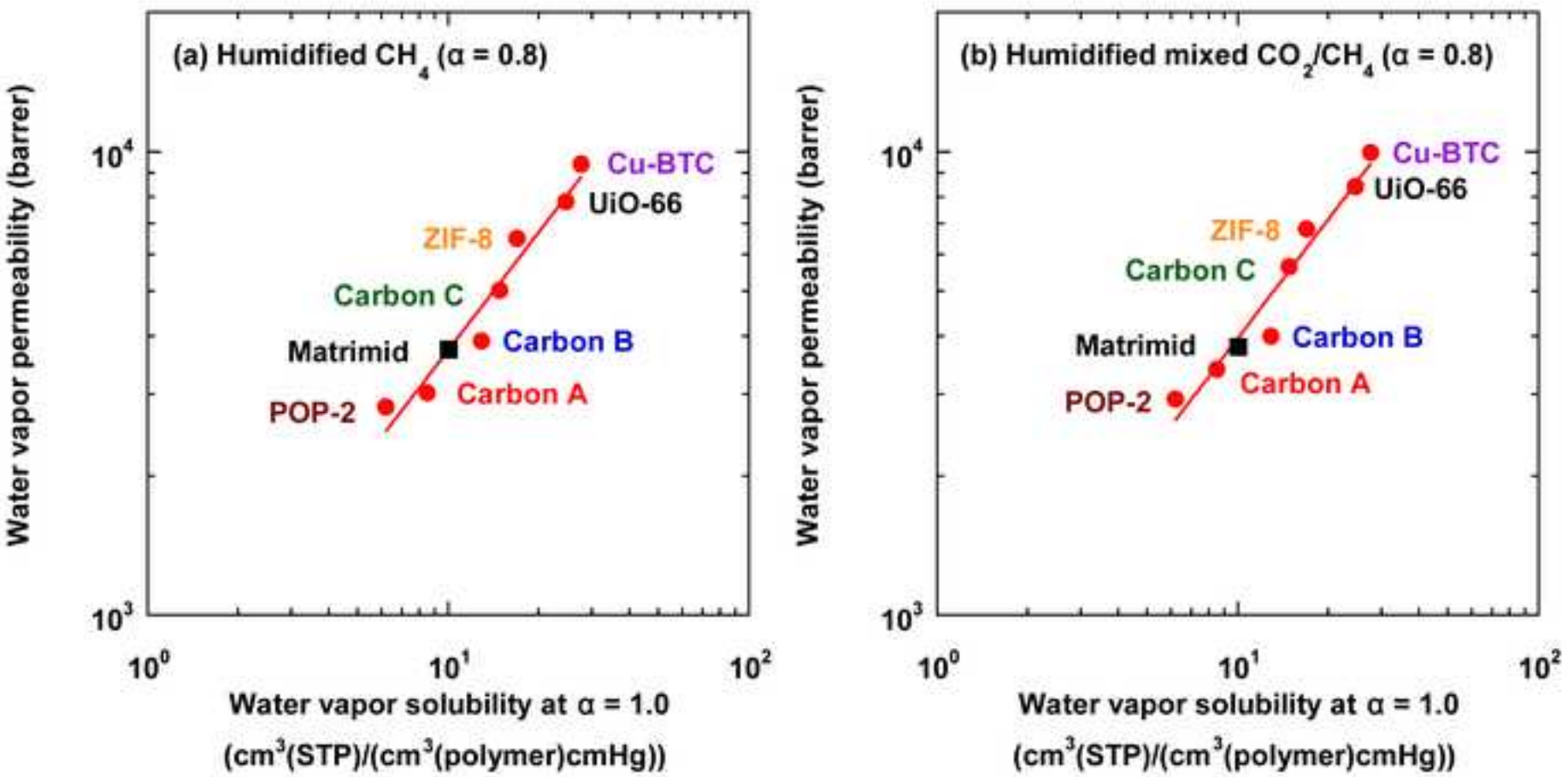

Figure 6

Click here to download high resolution image

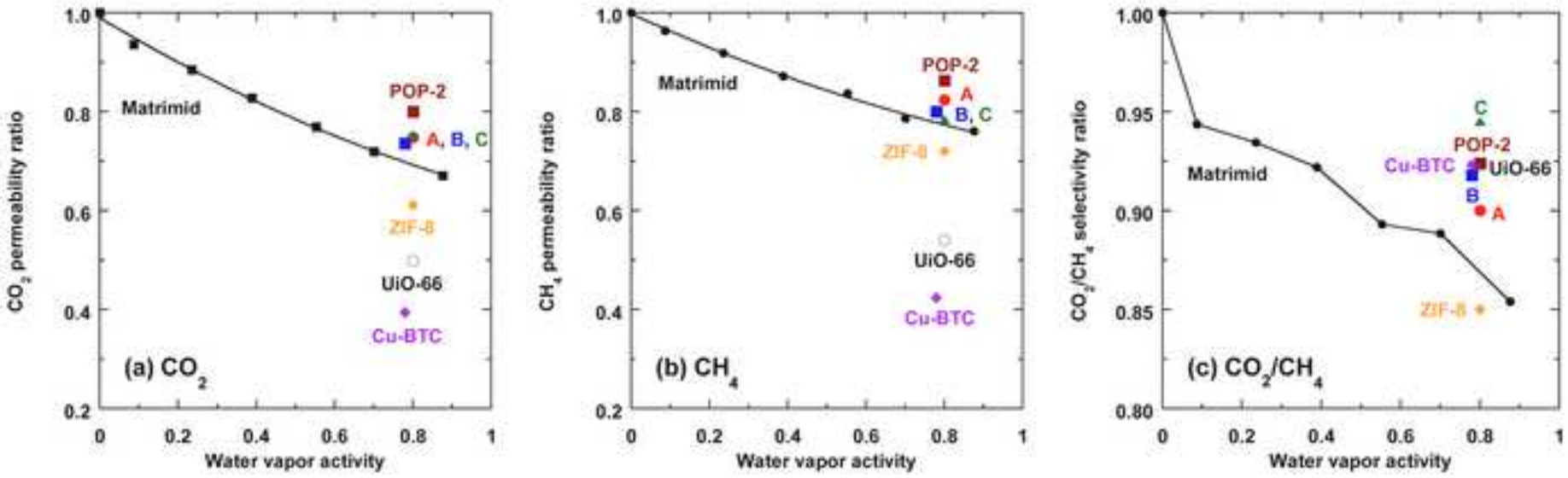

Figure 7

Click here to download high resolution image

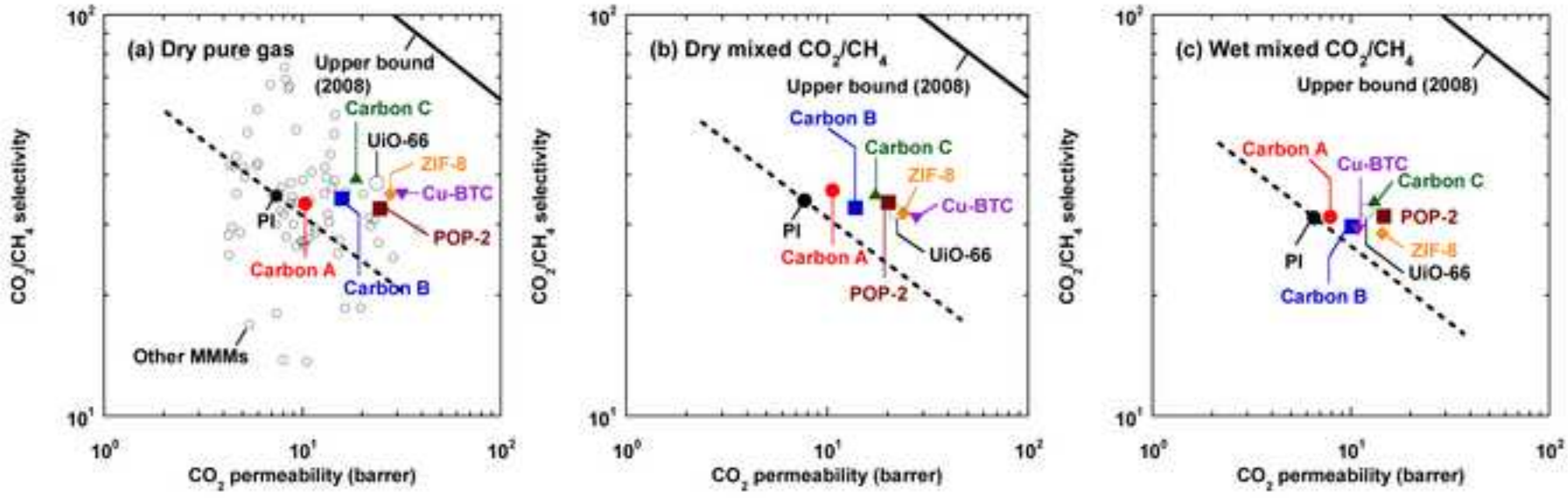

Table 1 Physical properties of the nanoparticles

Property	Carbon A	Carbon B	Carbon C	POP-2 [41]	UiO-66	ZIF-8	Cu-BTC
Type	Carbon	Carbon	Carbon	POP	MOF	MOF	MOF
Surface area (m^2/g) (a)	77	252	534	781	1267	1497±32	1725±150
Pore volume (cm^3/g) (a)	0.194	0.286	0.329	0.554	0.654	0.687±0.015	0.762±0.066
Particle size (nm) [60]	290	180	260	< 300	< 300	210	280
Absolute density (g/cm^3)	1.828 (b)	1.887 (b)	1.90	1.33	□	0.95 [33]	1.05±0.17 [54-56]
Fractional Free volume	0.35	0.54	0.63	0.74	□	0.65±0.02	0.80±0.07

(a) Determined from N_2 BET sorption analysis

(b) Cited from supplier information

Table 2 Physical properties of pure Matrimid and 20 wt% MMMs

Sample	Filler content (wt%)	Filler content (vol%)	Density (g/cm^3)	*FFV* [(a)]	Water uptake (wt%)
PI	0	0	1.223 ± 0.019	0.167	2.8 ± 0.4
Carbon A	20	14.3	1.297 ± 0.006	0.194	2.2 ± 0.5
Carbon B	20	13.9	1.301 ± 0.009	0.219	3.4 ± 0.5
Carbon C	20	13.9	1.276 ± 0.008	0.238	4.0 ± 0.2
POP-2	20	18.7	1.189 ± 0.008	0.273	1.9 ± 0.2
UiO-66	20	□	1.231 ± 0.005	□	6.8 ± 0.8
ZIF-8	20	24.3	1.147 ± 0.008	0.284	5.0 ± 0.2
Cu-BTC	20	20.3	1.207 ± 0.007	0.295	7.8 ± 0.3

(a) Determined from density data as per Kanehashi *et al.* [60]

Author/s:
Kanehashi, S; Chen, GQ; Ciddor, L; Chaffee, A; Kentish, SE

Title:
The impact of water vapor on CO2 separation performance of mixed matrix membranes

Date:
2015-10-05

Citation:
Kanehashi, S., Chen, G. Q., Ciddor, L., Chaffee, A. & Kentish, S. E. (2015). The impact of water vapor on CO2 separation performance of mixed matrix membranes. Journal of Membrane Science, 492, pp.471-477. https://doi.org/10.1016/j.memsci.2015.05.046.